Prediction of Viscous Coefficient of Venturi Meter under Non ISO Standard Conditions

Karthik Ms[1]
Department of Mechanical Engineering
Maharaja Institute of Technology,
Mysore

V Seshadri[2]
Professor,
Department of Mechanical Engineering
Maharaja Institute of Technology, Mysore

***Abstract*—Venturi meters are commonly used in single and multiphase flows. The ISO standard (ISO 5167-4) provides meter discharge coefficients for Venturi meters in turbulent flows with Reynolds numbers (Re) between 2×10^5 to 1×10^6, beta value (β) between 0.4 to 0.75 and diameter (D) between 50mm to 250mm . In viscous fluids, Venturi are sometimes operated in laminar flows at Reynolds numbers below the range covered by the standards. The focus of the study was directed towards very small Reynolds numbers commonly associated with pipeline transportation of viscous fluids. However high Reynolds number were also considered. The Computational Fluid Dynamics (CFD) program STAR CCM + was used to perform the research. Heavy oil and water were used separately as the two flowing fluids to obtain a wide range of Reynolds numbers with high precision. Multiple models were used with varying characteristics, such as pipe size and meter geometry, to obtain a better understanding of the C_d vs. Re relationship.**

Keywords - Venturi Meter, Computational Fluid Dynamics (CFD), Discharge Coefficient, Reynolds Number, Beta Value

I. INTRODUCTION

Among the differential pressure flow meter, Venturi Meter stands out and dominates in flow measurement field because of its simple and well understood concept, accurate and economical compared to other sophisticated flow meter. Still, study has been made to further understand the performance of Venturi Tube and its accuracy. Accurate flow measurement is one of the greatest concerns among many industries, because uncertainties in product flows can cost companies considerable profits. Differential pressure flow meters such as the Venturi, standard concentric orifice plate, V-cone, and wedge are popular for these applications at higher Reynolds numbers, because they are relatively inexpensive and produce reliable results. However, little is known about their discharge coefficient (C_d) values at low Reynolds numbers (Miller[1]) of the Venturi Meter. The calibrations for these meters are generally performed in a laboratory using cold water which, at low Reynolds numbers results in extremely small pressure differentials that are difficult to measure accurately. Consequently, there is a need for accurate low Reynolds number flow measurements for Venturi Meters. In the present work computational fluid dynamics techniques were utilized to characterize the behaviour of flow meters from very low to high Reynolds numbers. In particular, the CFD predictions of discharge coefficients were validated with results available in the literature. Results are presented in terms of predicted discharge coefficients. Reynolds numbers deserves excessive observation when it comes to analyzing the capabilities of Venturi Meter. The value of the Reynolds number for a particular pipe flow can be decreased by either decreasing the velocity, or increasing the viscosity. Thus a high viscosity fluid, heavy crude oil with a viscosity of 0.268 Pa-s is used.

Venturi Meter Discharge Coefficients

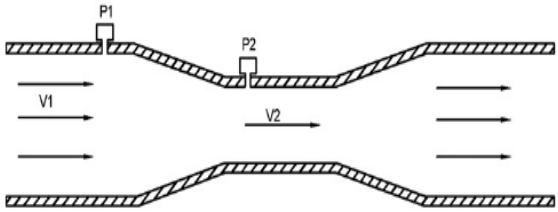

Fig-1: Venturi Meter

As Per ISO 5167-4 standard, the mass flow rate in a Venturi meter (q_m) is given by:

$$q_m = \frac{C_d}{\sqrt{1-\beta^4}} \frac{\pi d^2}{4} \sqrt{2(p_1 - p_2)\rho_1} \quad .....(1)$$

Where:

C_d	Venturi discharge coefficient
β	Venturi beta ratio, d/D
d	Venturi throat diameter, mm
D	Pipe diameter upstream of the Venturi convergent section, mm
p_1	Static pressure at the upstream pressure tap, Pa
p_2	Static pressure at the Venturi throat tap, Pa
ρ_1	Fluid density at the upstream tap location, Kg/mm^3

When working with Venturi meters, Reynolds numbers based on inlet pipe diameter (D) and throat diameter (d) are frequently used. These are defined as follows:

$$R_{e_D} = \frac{\rho v D}{\mu} .....(2a)$$

$$R_{ed} = \frac{\rho v d}{\mu} \quad \text{.....(2b)}$$

Where μ, ρ and v are the dynamic viscosity, density, and average velocity, corresponding to inlet pipe diameter (D) and throat diameter (d) respectively.

Equation (1) is based on the assumptions that include steady, incompressible, and in-viscid flow (no frictional pressure losses). Two of the assumptions that are inherent in the Venturi equation apply when metering viscous fluids under turbulent flow conditions. These are the assumptions that make the flow as turbulent, so the velocity profile is uniform across the cross-section, and that the frictional pressure losses within the meter can be neglected.

II. GEOMETRICAL MODEL

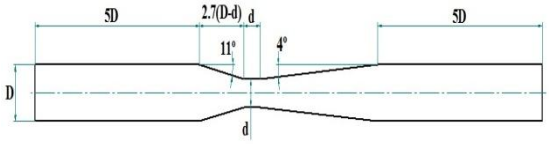

Fig-2.1: 2D Model

Fig-2.2: 3D Model

Fig-2.3: 2D Axis-Symmetric Model

The geometries of the Venturi Meter were constructed as per ISO-5167-4 standards. Venturi for 50 to 250mm diameter pipe at β values 0.4 to 0.75 with 5D upstream and 5D downstream of the Venturi have been modeled as shown in fig-2.1. the convergent section has been taken as 2.7 (D-d) length and 22^o included angle. throat length is same as the throat diameter d. whereas, the divergent section has taken as 8^o included angle.

III. NUMERICAL MODEL

CFD modelling is a useful tool to gain an insight into the physics of the flow and to help understand the test results. The CFD results were validated by running simulations for conditions within the range of the ISO standards and comparing the predicted discharge coefficients with the ISO standards values. Additional CFD simulations were conducted to predict discharge coefficient of Venturi meter at Reynolds numbers below the range covered by the standards.

The models were created and meshed in STAR CCM+. The geometries of the Venturi Meter were constructed as per ISO-5167-4 standards.

Fig-3: Meshed Model, Polyhedral Mesh

Once the geometry was constructed, the geometry is meshed with various elements like Tria, Quad and polyhedral elements. After the running the simulations for multiple meshing schemes, polyhedral cells were the best fit for the geometry and it is divided approximately into 50,000 cells.

Boundary Conditions:

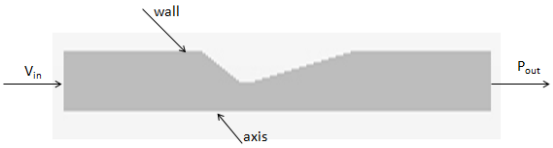

Fig-3.1: Boundary Conditions

Fig-3.1 shows the boundary conditions applied in STAR CCM+. The flow inlet on the 5-diameter upstream pipe was defined as the Velocity Inlet, The flow outlet on the 5-diameter downstream pipe was defined as a Pressure Outlet, all solid surfaces are treated as Wall. For 2D axis-symmetric studies central line has taken as Axis in simulation.

2D axis-symmetric model has been used for classical Venturi Meter, the process of grid generation is very crucial for accuracy, stability and economy of the prediction of coefficient of discharge. A fine grid leads to better accuracy and hence it is necessary to generate a reasonably fine grid in the region of steep velocity gradients. For efficient discretization the geometry was divided in to three parts, the upstream and downstream region and these were meshed with reasonably coarse grid whereas the central region containing the obstruction (convergent and divergent zone) and pressure taps was meshed with very fine grids in order to visualise the effect of obstruction geometry. The size of grid were kept very fine in the central region to account for the expected steep velocity gradients. The grid independence test were carried out by grid adaptation and comparing the value of C_d obtained with different grid density, it was found that grid density after 50000 had very less effect on C_d.

Viscous turbulence model considered for this study was the realizable k-epsilon model with the standard wall function enabled. This particular model was used for any of the

model that had a Reynolds(Re) number greater than 2,000. The laminar viscosity model was used for any of the models that had a Re of 2,000 or less. All the constants associated with this version of STAR CCM+ were left at their default values.

The study included heavy oil and water as the two different types of fluids to be examined in order to obtain data for the entire range of Reynolds numbers. Water was used for the larger Re(>20,000) while oil was used for the small Re numbers(<20,000). The primary difference between the two fluids was that the viscosity of the oil was much greater than that of water to ensure larger pressure differences at small Re. The velocity inlet condition only required the calculated velocity based on Reynolds numbers. The pressure outlet is set from 1-30 bar normal downstream pressures. It is important to observe when studying the results that potential cavitation is not taken into account using STAR CCM+ therefore high negative pressures are not a cause for concern.

The pressure velocity coupling used was the Simple Consistent algorithm. The Under-Relaxation Factors were set to 0.7 and 0.3 for velocity and pressure. Discretisation factors are vital when regarding the accuracy of the numerical results. For this study standard pressure was used, while the Second-Order Upwind method was applied for momentum, kinetic energy, and the turbulent dissipation rate.

Residual monitors were used to determine when a solution had converged to a point where the results had very little difference between successive iterations. When the k-epsilon model was applied, there were six different residuals being monitored which included: continuity, x, y, and z velocities, k, and epsilon. The study aimed to ensure the utmost iterative accuracy by requiring all of the residuals to converge to 1e-05, before the model runs were complete.

IV. RESULTS AND DISCUSSION

There are many pipelines where flows need to be accurately measured. Meters having a high level of accuracy and relatively low cost are a couple of the most important parameters when deciding on the purchase of a flow meter. Most differential pressure flow meters meet both of these requirements. Many of the most common flow meters have a specified range where the discharge coefficient may be considered constant and where the lower end is usually the minimum recommended R_e number that should be used with the specified meter. With the additional knowledge of this study it will enable the user to better estimate the flow through a pipeline over a wider range of Reynolds numbers. The research completed in this study on discharge coefficients focused on Venturi Meter with varying beta ratios and diameters.

It was seen that the best way to present the data for interpretation is by using semi-log graphs for plotting discharge coefficient vs. Reynolds number. Each of the data points on the graphs was computed separately based on the performance from a Reynolds number. The velocities that were needed to obtain different Reynolds number values were the primary variable put into the numerical model when computing each discharge coefficients. Heavy Oil was used for flows where Re < 20,000 while water was used for higher turbulent flow test runs.

Venturi flow meter models were created to determine their discharge coefficient for a wide range of Reynolds numbers. The different β values used for the models were 0.661and 0.5 with diameters of 230mm and154.1mm to observe if there was any significant difference in results based on pipe diameter.

The Venturi meter was modelled using different geometries to determine if there was significant effect on the resultant C_d over the Re range. It was found that the data sets followed very similar trends despite having different geometries.

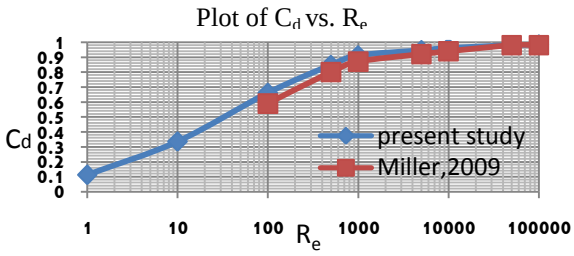

Fig-4: comparison of present study vs. miller physical study.

Re	C_d	
	Present Study	Miller,2009
100000	0.985	0.98
50000	0.98	0.98
10000	0.96	0.94
5000	0.945	0.92
1000	0.912	0.87
500	0.848	0.8
100	0.661	0.59
10	0.336	
1	0.112	

Table-1: comparison of present study vs. miller physical study.

As illustrated in the fig-4 the simulation presented in the present work were in close agreement with the Miller[1] experimental values for the Reynolds number ranging from 100 to 1,00,000. Miller[1,] used a multiphase flow of heavy oil and water through the Venturi meters tested, which may be the reason that the C_d values decrease more rapidly than the present study. the multiphase flow was not completely

mixed, some of the oil may settle at the entrance of the Ventrui Meter.

Table-2: For Standard Conditions (Re=5,00,000)

Beta(β)	C_d	
	D=230mm	D=154.1mm
0.661	0.9925	0.9955
0.5	0.996	0.996

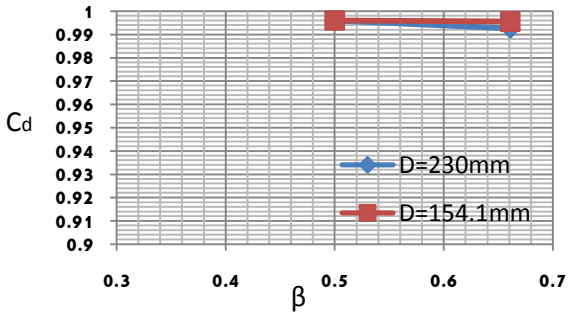

Fig-4.1: Venturi Discharge Coefficients For Standard Conditions.

Fig 4.1. shows the Venturi discharge coefficient for standard conditions. In these simulation the result show that the discharge coefficients for different diameter with varying beta values becomes constant. C_d values is around 0.99.

Table-3: For Non Standard Condition(D=154.1mm)

[Re]	C_d	
	β=0.661	β=0.5
100000	0.985	0.988
50000	0.980	0.982
10000	0.960	0.967
5000	0.945	0.950
1000	0.912	0.896
500	0.848	0.847
100	0.661	0.679
10	0.336	0.382
1	0.112	0.143

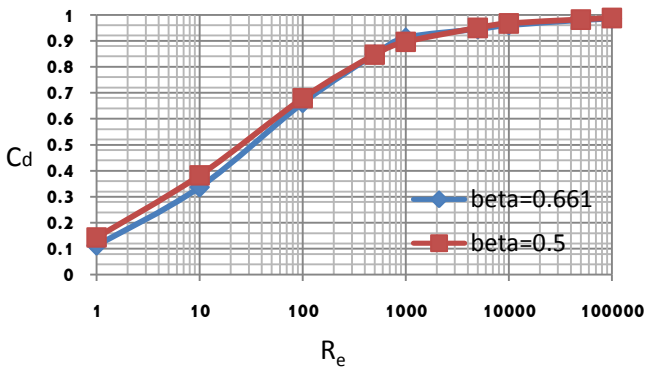

Fig-4.2: Venturi discharge coefficients for Non standard conditions (D=154.1mm).

Table-4: For Non Standard Condition (D=230mm)

[Re]	C_d	
	β=0.661	β=0.5
100000	0.985	0.987
50000	0.982	0.985
10000	0.956	0.966
5000	0.939	0.949
1000	0.905	0.894
500	0.843	0.840
100	0.659	0.695
10	0.339	0.390
1	0.120	0.144

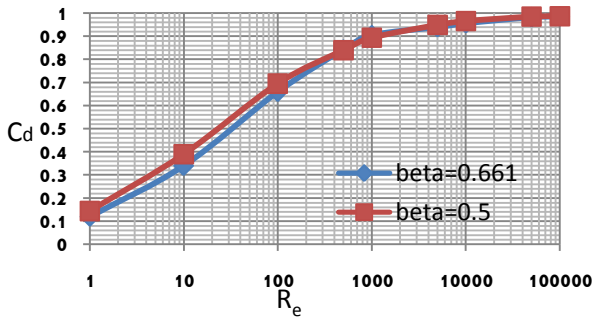

Fig-4.3: Venturi discharge coefficients for Non standard conditions (D=230 mm).

The Venturi meter was modeled different geometries to determine if there was significant effect on the coefficient of discharge over the varying Reynolds number. it was found that all the data sets followed very similar trends. As the Reynolds numbers went from 1,00,000 to 1, the coefficient of discharge values dropped from 0.98 to 0.1 on the semi-log plot shown in Fig- 4.2 and 4.3.

Pressure and Velocity Contours.

For Standard Conditions[Re=5,00,000]

Diameter = 154.1mm

Beta Value = 0.5

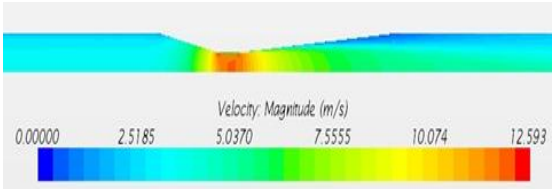

Fig-4.4a Venturi Velocity Contours.

The velocity contour is as shown in Fig-4.4a The velocity magnitude is increase as we move from upstream tap to throat tap. The velocity at the upstream tap is 2.89m/s. The velocity at the throat tap is 10.159m/s.

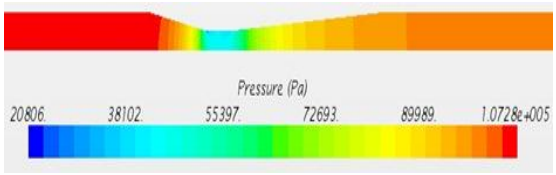

Fig-4.4b. Venturi Pressure Contours.

The pressure contour is as shown in Fig-4.4b. The pressure is decreases as we move from upstream tap to throat tap. The pressure at the upstream tap is 106901.4pa. The pressure at the throat tap is 42684.4pa.

For Diameter = 230mm
Beta Value = 0.661

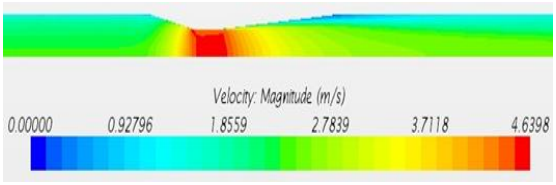

Fig-4.4c. Venturi Velocity Contours.

The velocity contour is as shown in Fig-4.4c. The velocity magnitude is increase as we move from upstream tap to throat tap. The velocity at the upstream tap is 1.935m/s. The velocity at the throat tap is 4.428m/s.

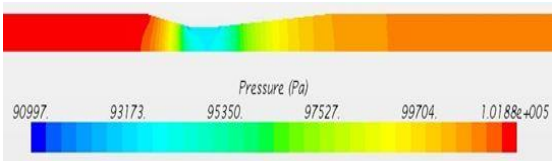

Fig-4.4d. Venturi Pressure Contours.

The pressure contour is as shown in Fig-4.4d. The pressure is decreases as we move from upstream tap to throat tap. The pressure at the upstream tap is 101715.4pa. The pressure at the throat tap is 93661.7pa.

For Non Standard Conditions

Diameter = 230mm
Beta Value = 0.661 , Re=100000

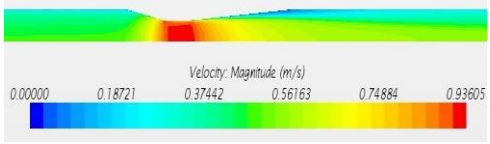

Fig-4.4e. Venturi Velocity Contours.

The velocity contour is as shown in Fig-4.4e. The velocity magnitude is increase as we move from upstream tap to throat tap. The velocity at the upstream tap is 0.387m/s. The velocity at the throat tap is 0.885m/s.

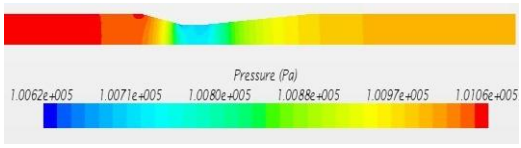

Fig-4.4f. Venturi Pressure Contours.

The pressure contour is as shown in Fig-4.4f. The pressure is decreases as we move from upstream tap to throat tap. The pressure at the upstream tap is 101045.2pa. The pressure at the throat tap is 100718.6pa.

For Diameter = 230mm
Beta Value = 0.661 , Re=1

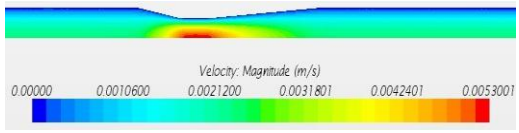

Fig-4.4g. Venturi Velocity Contours.

The velocity contour is as shown in Fig-4.4g. The velocity magnitude is increase as we move from upstream tap to throat tap. The velocity at the upstream tap is 0.00116m/s. The velocity at the throat tap is 0.00266m/s.

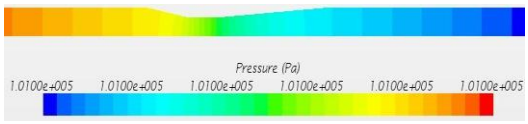

Fig-4.4h. Venturi Pressure Contours.

The pressure contour is as shown in Fig-4.4h. The pressure is decreases as we move from upstream tap to throat tap. The pressure at the upstream tap is 101000.7pa. The pressure at the throat tap is 101000.5pa.

For Diameter = 230mm
Beta Value = 0.5 , Re=100000

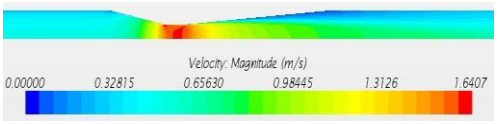

Fig-4.4i. Venturi Velocity Contours.

The velocity contour is as shown in Fig-4.4i. The velocity magnitude is increase as we move from upstream tap to throat tap. The velocity at the upstream tap is 0.387m/s. The velocity at the throat tap is 1.548m/s.

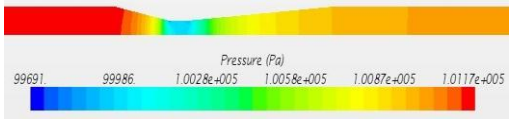

Fig-4.4j. Venturi Pressure Contours.

The pressure contour is as shown in Fig-4.4j. The pressure is decreases as we move from upstream tap to throat tap. The pressure at the upstream tap is 101152.2pa. The pressure at the throat tap is 99985.26pa.

For Diameter = 230mm
Beta Value = 0.5, Re=1

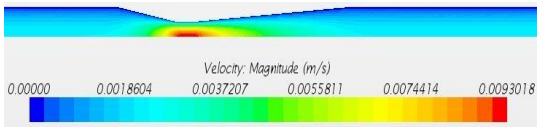

Fig-4.4k Venturi Velocity Contours.

The velocity contour is as shown in Fig-4.4k. The velocity magnitude is increase as we move from upstream tap to throat tap. The velocity at the upstream tap is 0.00116m/s. the velocity at the throat tap is 0.004658m/s.

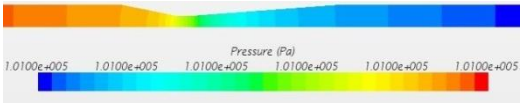

Fig-4.4k. Venturi Pressure Contours.

The pressure contour is as shown in Fig-4.4k. The pressure is decreases as we move from upstream tap to throat tap. The pressure at the upstream tap is 101001.6pa. the pressure at The throat tap is 101001.1pa.

V. CONCLUSION

The CFD program STAR CCM+ was used to create multiple models in an effort to understand trends in the discharge coefficients for Venturi Meter with varying Reynolds numbers. The research established the discharge coefficient for Re numbers ranging from 1 to 5,00,000. For turbulent flow regimes water was modelled as the flowing fluid, while for laminar flow ranges heavy oil was modelled to create larger viscosities resulting in smaller Re. The range of Reynolds numbers for which physical data was obtained is small in comparison to the range of data obtained using computational fluid dynamics techniques. The use of Computational Fluid Dynamics aids in the ability to replicate this study while minimizing human errors. The data from this study demonstrates that with possible discharge coefficients near 0.15 .the iterative process be used to minimize flow rate errors.

Different graphs were developed to present the results of the research. These graphs can be used by readers to determine how Venturi Meter performance may be characterized for pipeline flows for varying viscosities of non-compressible fluids. The results from this study could be expanded with future research of discharge coefficients of Venturi Meters. An area of potential interest is performing tests over a wide range of beta values and different diameter of Eccentric type of Venturi Meters and Rectangular type of Venturi Meters to obtain a more complete understanding of discharge coefficient relationship.

REFERENCES

[1] ISO 5167-4, "Measurement of Fluid Flow by Means of Pressure Differential Devices Inserted in Circular Cross-Section Conduits Running Full – Part 4: Venturi Tubes," 2003.
[2] Gordon Stobie, ConocoPhillips Robert Hart and Steve Svedeman, Southwest Research Institute® Klaus Zanker, Letton-Hall Group. Erosion in a Venturi Meter with Laminar and Turbulent Flow and Low Reynolds Number Discharge Coefficient Measurements.
[3] Miller Pinguet B, Theuveny B, Mosknes P, 2009. The Influence of Liquid Viscosity on Multiphase Flow Meters, TUVNEL, Glasgow, United Kingdom.
[4] Hollingshead C.L, Johnson M.C, Barfuss S.L, Spall R.E. 2011. Discharge coefficient performance of Venturi, standard concentric orifice plate, V-cone and wedge flow meters at low Reynolds numbers. Journal of Petroleum Science and Engineering .
[5] Discharge coefficients of Venturi tubes with standard and non standard convergent angles by M.J. Reader-Harris W.C.Brunton, J.J.Gibson, D.Hodges, I.G. Nicholson.
[6] Optimization of Venturi Flow Meter Model for the Angle of Divergence with Minimal Pressure Drop by Computational Fluid Dynamics Method by T. Nithin, Nikhil Jain and Adarsha Hiriyannaiah.
[7] CFD Analysis Of Permanent Pressure Loss For Different Types Of Flow Meters In Industrial Applications C. B. Prajapati, V. Seshadri, S.N. Singh, V.K. Patel.
[8] Miller, R. W., Flow Measurement Engineering Handbook, McGraw-Hill, New York, 1996.
[9] Fox, R. W., and McDonald, A. T., Introduction to Fluid Mechanics, Wiley and Sons, New York, 1992.